Acta Cryst. (1974). B**30**, 1412

New Refinements of the γ Brass Type Structures Cu_5Zn_8, Cu_5Cd_8 and Fe_3Zn_{10}

BY J. K. BRANDON, R. Y. BRIZARD, P. C. CHIEH, R. K. MCMILLAN AND W. B. PEARSON
Faculty of Science, University of Waterloo, Waterloo, Ontario, Canada

(*Received* 22 *November* 1972; *accepted* 3 *January* 1974)

The crystal structures of Cu_5Zn_8, Cu_5Cd_8 and Fe_3Zn_{10} have been studied using single-crystal X-ray diffraction techniques. All three alloys have the body-centred cubic space group $I\bar{4}3m$ with four formula units per unit cell. Lattice parameters are 8·878 (4), 9·615 (10) and 9·018 (3) Å respectively for Cu_5Zn_8, Cu_5Cd_8 and the pseudocell of Fe_3Zn_{10}. Evidence shows a new superstructure of 36 Å at the composition Fe_3Zn_{10}. Values of lattice parameter as a function of composition are given for the Cu_5Cd_8 phase. New data are presented on the three structures, and the ordering of the atomic species is compared with that reported by previous workers. Significant differences in our ordering for Fe_3Zn_{10} are attributed to our different composition within the γ phase. X-ray diffraction intensity data were collected using a 3-circle automatic single-crystal diffractometer and Mo *Kα* X-radiation. The crystal structures were refined using full-matrix least-squares methods to final *R* values of 6·1 %, 7·5 %, and 5·5 % respectively. A discussion of possible reinterpretations for these and other γ brass structures is presented.

Introduction

The structure determinations reported here were undertaken as the first part of a programme of study on γ brass related structures. Later reports will cover our results on related γ structures known to fall into several categories such as ordered superstructures, defect structures incorporating vacancies, and defect structures showing a loss of cubic symmetry. The archetype γ brass structure is the basis for all of these, and it has received considerable theoretical attention because it occurs in many binary and ternary alloy systems close to the rather well defined value $\frac{21}{13}$ for the ratio e/a (number of valence electrons per atom averaged over the contents of a unit cell).

Early work on γ brass structures (Westgren & Phragmén, 1925; Bradley & Thewlis, 1926; Bradley & Gregory, 1931) has shown the archetype to possess a body-centred cubic cell containing 52 atoms with a cell constant $a \simeq 9$ Å and space group $I\bar{4}3m$ (T_d^3, No. 217). Early papers described γ brass as an array of 27 3 Å body-centred cubes with two atoms missing at the corners and body centre of the resulting 9 Å cube and with other atoms slightly displaced. Bradley & Jones (1933) described γ structures in terms of clusters of atoms, each containing 26 atoms, centred at the corners and body centres of the 9 Å cubes. We prefer to use the cluster description of Bradley & Jones. This viewpoint has also been adopted by other investigators of the γ type structures (Westman, 1965).

The idealized cluster (see Fig. 1) can be viewed as 26 atoms occupying four different types of geometrical sites building outward from the centre: (1) four atoms forming an inner tetrahedron (IT); (2) four atoms forming an outer tetrahedron (OT) such that each OT atom touches three IT atoms; (3) six atoms forming an octahedron (OH) such that each OH atom is a neighbour of two IT and two OT atoms; and (4) twelve atoms forming a cubo-octahedron (CO) such that each CO atom is a close neighbour of one IT, one OT and two OH atoms and a slightly more distant neighbour of two CO atoms. The precise description of any actual cluster and questions of its stability naturally depend on the sizes of metal atom species on the various IT, OT, OH and CO sites, and possibly on the extent to which any atom type may distort from spherical shape. A detailed discussion of the appropriateness of the cluster in achieving overall packing efficiency both within clusters and between neighbouring clusters is presented elsewhere (Brandon, Chieh, Pearson & Riley, 1974).

When we began single-crystal examinations of γ type structures, the only other single-crystal study of which we were aware was that of Cu_9Al_4 by Westman (1965). After refining our data on Cu_5Zn_8, Cu_5Cd_8 and our pseudocell Fe_3Zn_{10} structures, we became aware of the further work by Heidenstam, Johansson & Westman (1968) and by Johansson, Ljung & Westman (1968) on γ type structures. A comparison is made between the results of our new studies, based on considerably more data, and their results.

Experimental

Single crystals of Cu_5Zn_8 and Cu_5Cd_8 were obtained from alloys made from pure metals and finally annealed at 797 and 538 ± 5°C respectively. Single crystals of Fe_3Zn_{10} (containing approximately 24 at.% Fe) were isolated by acid dissolution of a Zn-rich ingot (containing approximately 92 at.% Zn) which was slowly cooled from 805 to 680°C and then quenched in water.

Good-quality single crystals were selected from each sample by inspection of their X-ray diffraction photographs. These photographs provided approximate cell constants and indicated Laue class *m*3*m* with systematic absences for reflexions with $h+k+l$ odd allowing possible space groups $I432$ (No. 211), $I\bar{4}3m$ (No. 217), and $Im3m$ (No. 229). Density measurements indicated $Z=4$ formula units per unit cell in each of the alloys. In the case of γ Fe–Zn, both photographs (Cu $K\alpha$) and diffractometer (Mo $K\alpha$) measurements for several different crystals indicated the existence of weak reflexions consistent with a cubic superlattice of four times the basic 9 Å cell edge.

The crystals selected for diffraction intensity measurements had mean diameters of 0·26, 0·13 and 0·10 mm for Cu_5Zn_8, Cu_5Cd_8 and Fe_3Zn_{10} respectively. Their shapes were slightly irregular cubes or irregular cylinders. Average absorption coefficients μR for Mo $K\alpha$ radiation were calculated to be 5·6 for γ Cu–Zn, 2·0 for γ Cu–Cd, and 1·9 for γ Fe–Zn. Accurate cell constants were determined at 23°C by least-squares analysis of measured 2θ values obtained using Zr-filtered Mo $K\alpha$ radiation ($\lambda_{K\bar{\alpha}}=0{\cdot}71069$ Å) on a General Electric XRD-6 three-circle single-crystal diffractometer. The intensities of reflexions were measured on this same instrument using a scintillation counter and pulse-height analyser with Mo $K\alpha$ radiation and an ω–2θ scan. Data were corrected for Lorentz and polarization effects, and for each sample absorption corrections were applied according to approximate spherical or cylindrical shapes. For γ Fe–Zn, intensities were measured on the 9·018 Å cubic cell in order to determine the average subcell structure.

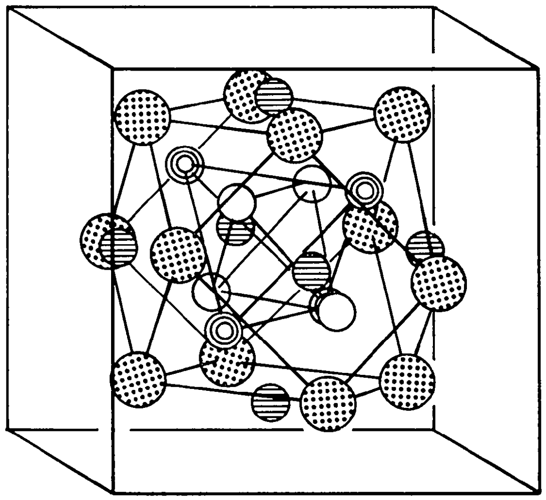

Fig. 1. Cluster of 26 atoms in the γ brass structure (after Heidenstam, Johannson & Westman, 1968). Open circles: inner tetrahedron, IT. Concentric circles: outer tetrahedron, OT. Cross-hatched circles: octahedron, OH. Dotted circles: cubo-octahedron, CO.

Compositions of the Cu_5Zn_8 and Cu_5Cd_8 single crystals were determined from lattice-parameter data, and that of the Fe_3Zn_{10} crystal was determined from the γ phase boundary and the temperature of the molten Zn-rich alloy from which it was obtained. The lattice parameter which we obtained for the Fe_3Zn_{10} single crystal, together with the lattice-parameter measurements of Schramm (1938), since confirmed by Johansson, Ljung & Westman (1968), agree with the composition of approximately 24 at.% Fe for our crystal.

Since data for the variation of lattice parameter with composition for γ Cu–Cd were unavailable, powders of several two-phase alloys containing γ phases were quenched from various temperatures so that the γ compositions could be derived from the known boundaries of the γ phase. The lattice parameters were determined from X-ray photographs in a 114·6 mm diameter Norelco powder diffraction camera, and the resulting lattice parameter *vs.* composition data given in Table 1 were used to determine the composition of the single crystal. The data for γ Cu–Cd show a linear variation of a with atomic percentage Cd. The increase in a per at.% composition for γ Cu–Zn (data of Owen & Pickup, 1933, and Johansson & Westgren, 1933) and γ Cu–Cd is a linear function of the atomic volumes of Cu, Zn and Cd.

Structure determinations and refinements

Starting models for all three alloy structures were derived from the early model of archetype γ brass. The models were refined by full-matrix least-squares methods using the program *LSTSQR* (a modified version by Doedens and Ibers of *ORFLS*, Oak Ridge full-matrix least-squares program) on the IBM 360/75 computer at the University of Waterloo. The atomic scattering factors were interpolated from data in *International Tables for X-ray Crystallography* (1968) taking the Thomas–Fermi–Dirac statistical model values for γ Cu–Cd and the self-consistent wave function model values for γ Cu–Zn and γ Fe–Zn. Corrections for anomalous scattering were made. In the final stages of

Table 1. γ Cu–Cd *lattice parameters*

Composition from phase boundaries* (at.% Cd)	Lattice parameter a (Å)	X-ray samples		
		Phases	Composition (at.% Cd)	Quenching temperature (°C)
54·5	9·540	$\gamma+Cu_4Cd_3$	53·0	538
56·7	9·571	$\gamma+Cu_4Cd_3$	53·0	451
61·2	9·626	γ+liquid	65·1	538
63·0	9·657	γ+liquid	65·1	451
63·0	9·658	γ+liquid	74·1	451

* From Hansen (1958)

Table 2. *Comparison of recent structural data for the γ-brass structure*

		Cu_5Zn_8		Cu_5Cd_8		Fe_3Zn_{10}		
Reference		Heidenstam *et al.* (1968)	This work	Heidenstam *et al.* (1968)	This work	Johansson *et al.* (1968)		This work
Sample		Powder	Single crystal 64·8 % Zn	Single crystal	Single crystal 60 % Cd	Single crystal 29·5 % Fe	Powder 29·5 % Fe	Single crystal 24 % Fe
		$Cu_{20}Zn_{32}$	$Cu_{18.3}Zn_{33.7}$	$Cu_{20}Cd_{32}$	$Cu_{20.8}Cd_{31.2}$	$Fe_{16}Zn_{36}$	$Fe_{16}Zn_{36}$	$Fe_{12.5}Zn_{39.5}$
Radiation used		Neutron (λ = 1·07 Å)	Zr-filtered Mo $K\alpha$	Ni-filtered Cu $K\alpha$	Zr-filtered Mo $K\alpha$	Ni-filtered Cu $K\alpha$	Neutron (λ = 1·07 Å)	Zr-filtered Mo $K\alpha$
Cell constant (Å)		8·869 ± 2	8·878 ± 4	9·5888 ± 3	9·615 ± 10	8·9822 ± 12		9·018 ± 3§
Space group		$I\bar{4}3m$	$I\bar{4}3m$	$I\bar{4}3m$	$I\bar{4}3m$	$I\bar{4}3m$	$I\bar{4}3m$	$I\bar{4}3m$
Atom positions and temperature factors								
IT 8(*c*) (*xxx*)	$x \pm \sigma$	0·110 ± 3*	0·1089 ± 5	0·0939 ± 11	0·0940 ± 6	0·0973 ± 15		0·1028 ± 5
	$B \pm \sigma$	1	1·12 ± 8	1·1 ± 4	0·73 ± 10	2·8 ± 5		0·98 ± 7
OT 8(*c*) (*xxx*)	$x \pm \sigma$	−0·172 ± 3	−0·1720 ± 4	−0·1617 ± 12	−0·1607 ± 7	−0·1638 ± 13		−0·1673 ± 4
	$B \pm \sigma$	1	0·88 ± 8	1·2 ± 4	0·74 ± 9	3·3 ± 5		0·52 ± 7
OH 12(*e*) (*x*00)	$x \pm \sigma$	0·355 ± 3	0·3558 ± 4	0·3506 ± 9	0·3514 ± 4	0·3551 ± 15		0·3538 ± 4
	$B \pm \sigma$	1	0·71 ± 6	2·0 ± 2	1·07 ± 7	2·3 ± 4		0·94 ± 6
CO 24(*g*) (*xxz*)	$x \pm \sigma$	0·313 ± 3	0·3128 ± 3	0·2980 ± 5	0·2974 ± 2	0·3029 ± 8		0·3045 ± 2
	$z \pm \sigma$	0·036 ± 3	0·0366 ± 4	0·0577 ± 7	0·0569 ± 3	0·0508 ± 12		0·0491 ± 3
	$B \pm \sigma$	1	1·32 ± 6	1·6 ± 2	1·15 ± 6	3·1 ± 4		1·13 ± 5
Site occupancy								
IT		Zn	Zn†	Cu	Cu	Fe	Fe	4Fe + 4Zn
OT		Cu	Cu†	Cu	Cu	Zn	Zn	Fe
OH		Cu	Cu†	10·7 Cd + 1·3 Cu	9 Cd + 3 Cu	8 Fe + 4 Zn	8 Fe + 4 Zn	Zn
CO		Zn	Zn†	21·3 Cd + 2·7 Cu	22 Cd + 2 Cu	Zn	Zn	Zn
R		–	6·1 %	11 %	7·5 %	11 %	7 %‡	5·5 %
Number of independent reflexions used in refinement		23	158	80	194	66	15	183

* Data of Bradley & Gregory (1931).
† See text for discussion of these occupancies.
‡ *R* quoted for intensities, not structure amplitudes.
§ Pseudo-cell.

least-squares refinement, a Cruickshank weighting scheme was used for each structure.

For Cu_5Zn_8 our refinement gave an R of 6·1% for the ordering of Bradley & Gregory (1931) with Zn on IT and CO sites and Cu on OT and OH sites ($R = \{\sum ||F_o| - |F_c|| / \sum |F_o|\} \times 100\%$, summations over the observed reflexions).

For Cu_5Cd_8 the occupancy of OH and CO sites was determined by separate refinements with various Cu to Cd ratios, and a small number of Cu atoms on these positions was indicated. Refinement of the composition of the other positions gave no indication of any Cd on the IT or OT sites. The lowest R value obtained was 7·5%.

For Fe_3Zn_{10}, similar refinements of our data with various compositions led to a lowest R value of 5·5% with a model containing equal numbers of Fe and Zn on IT sites, Fe on OT sites, and Zn on OH and CO sites.

During refinement cycles run to test alternative compositions among the sites, isotropic temperature factors were allowed to vary. Models for which any individual isotropic temperature factors became rather large ($B > 1·5$) or rather small ($B < 0·5$) were regarded as less realistic because thermal parameters might compensate for the chosen scattering factor on any particular site. The largest isotropic temperature factors for the three structures tend to occur for the atoms with largest scattering factor, possibly indicating more randomization of species on all sites. On the other hand the largest isotropic temperature factor in each structure occurs for the CO sites which are, on the cluster model, much less rigidly confined by their inter-cluster and intra-cluster neighbours. Larger thermal motions could indeed be anticipated for these sites on the boundaries of each cluster.

Table 2 summarizes our crystal data and refined structural parameters, and gives a comparison of our results and other reported data. Table 3 contains our interatomic distances around each crystallographic site, listed in corresponding order for the three alloys.

Table 4. *Structure-factor tables for* Cu_5Zn_8, Cu_5Cd_8 *and* Fe_3Zn_{10}

h, k, l, $|F_o|$, $|F_c|$, and α are listed. α appears in units of millicycles.

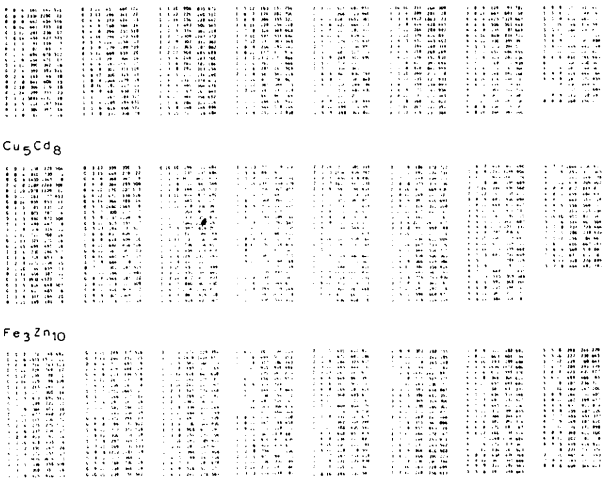

Table 3. *Interatomic distances in* Cu_5Zn_8, Cu_5Cd_8 *and* Fe_3Zn_{10} (Å)

Standard error is typically ±0·03 Å. A primed symbol denotes an atom in a different cluster.

Cu_5Zn_8			Cu_5Cd_8			Fe_3Zn_{10}		
IT (Zn)–IT (Zn)	3	2·74	IT (Cu)–IT (Cu)	3	2·56	IT (Fe/Zn)–IT (Fe/Zn)	3	2·62
–OT (Cu)	3	2·62	–OT (Cu)	3	2·61	–OT (Fe)	3	2·57
–OH (Cu)	3	2·58	–OH (Cd/Cu)	3	2·79	–OH (Zn)	3	2·62
–CO (Zn)	3	2·64	–CO (Cd/Cu)	3	2·79	–CO (Zn)	3	2·62
–OT′ (Cu)	1	3·37	–OT′ (Cu)	1	4·08	–OT′ (Fe)	1	3·59
OT (Cu)–IT (Zn)	3	2·62	OT (Cu)–IT (Cu)	3	2·61	OT (Fe)–IT (Fe/Zn)	3	2·57
–OH (Cu)	3	2·71	–OH (Cd/Cu)	3	2·85	–OH (Zn)	3	2·72
–CO (Zn)	3	2·56	–CO (Cd/Cu)	3	2·80	–CO (Zn)	3	2·62
–CO′ (Zn)	3	2·59	–CO′ (Cd/Cu)	3	2·77	–CO′ (Zn)	3	2·58
–IT′ (Zn)	1	3·37	–IT′ (Cu)	1	4·08	–IT′ (Fe/Zn)	1	3·59
OH (Cu)–IT (Zn)	2	2·58	OH (Cd/Cu)–IT (Cu)	2	2·79	OH (Zn)–IT (Fe/Zn)	2	2·62
–OT (Cu)	2	2·71	–OT(Cu)	2	2·85	–OT (Fe)	2	2·72
–OH′ (Cu)	1	2·56	–OH′ (Cd/Cu)	1	2·86	–OH′ (Zn)	1	2·64
–CO (Zn)	4	2·82	–CO (Cd/Cu)	4	2·96	–CO (Zn)	4	2·82
–CO′ (Zn)	2	2·54	–CO′ (Cd/Cu)	2	2·89	–CO′ (Zn)	2	2·64
–CO′ (Zn)	2	2·85	–CO′ (Cd/Cu)	2	3·39	–CO′ (Zn)	2	3·05
CO (Zn)–IT (Zn)	1	2·64	CO (Cd/Cu)–IT (Cu)	1	2·79	CO (Zn)–IT (Fe/Zn)	1	2·62
–OT (Cu)	1	2·56	–OT (Cu)	1	2·80	–OT (Fe)	1	2·62
–OT′ (Cu)	1	2·59	–OT′ (Cu)	1	2·77	–OT′ (Fe)	1	2·58
–OH (Cu)	2	2·82	–OH (Cd/Cu)	2	2·96	–OH (Zn)	2	2·82
–OH′ (Cu)	1	2·54	–OH′ (Cd/Cu)	1	2·89	–OH′ (Zn)	1	2·64
–OH′ (Cu)	1	2·85	–OH′ (Cd/Cu)	1	3·39	–OH′ (Zn)	1	3·05
–CO (Zn)	2	3·47	–CO (Cd/Cu)	2	3·27	–CO (Zn)	2	3·26
–CO′ (Zn)	4	2·64	–CO′ (Cd/Cu)	4	3·00	–CO′ (Zn)	4	2·75
–CO′ (Zn)	2	3·39	–CO′ (Cd/Cu)	2	4·05	–CO′ (Zn)	2	3·64

Table 4 gives our observed and calculated structure factor data for the observable reflexions in each of the three refinements. Calculated phase angles are in units of millicycles.

Discussion

Table 2 shows general agreement with earlier results for the atomic coordinates and the site occupancies in our refinements of Cu_5Zn_8 and Cu_5Cd_8. Our data show improved R values for considerably larger numbers of measured structure amplitudes.

In the case of Cu_5Zn_8, it was observed that an R value of 5·9% could be obtained for a model structure with nearly identical atomic coordinates but with Cu in IT and OT sites and Cu and Zn randomly in OH and CO sites. Although this model refined to a slightly lower R value than the one (6·1%) with atom distributions proposed by Bradley & Gregory (1931) from powder work and recently by Heidenstam, Johansson & Westman (1968), we have rejected it on the basis of interatomic distances. In particular the intercluster OH–OH′ distance of 2·56 Å indicates that Cu occupies the OH sites, and the intracluster IT–IT distance of 2·74 Å indicates that Zn occupies the IT sites (accepted metallic diameter for Cu $\simeq$ 2·56 Å and for Zn $\simeq$ 2·76 Å). The slightly lower R value of 5·9% is not significant and probably can occur because the atomic scattering factors of Cu and Zn are so similar and slight variations in isotropic temperature factors can compensate for small differences in scattering factors. Hence R is a poor indicator of actual Cu and Zn distributions in Cu_5Zn_8 compared with arguments which use relatively well known atomic radii to fit the observed interatomic distances in those parts of the cluster which are expected to pack tightly.

In the case of Cu_5Cd_8, Table 2 shows that a slightly higher Cu content was found on the OH sites in our sample. Our refinement of this occupancy for various Cu to Cd ratios leads us to suggest that the OH sites may be preferentially accepting additional Cu atoms as the composition varies toward higher atomic percentage of Cu within the γ phase region.

The refined structure of Fe_3Zn_{10} assuming a 52-atom pseudo-cell gave different results from those presented by Johansson, Ljung & Westman (1968). We suggest that these differences are real and reflect the different compositions of the samples examined. Our sample contains 12 Fe atoms whereas that of Johanssen *et al.* (1968) contains 16 Fe atoms per 52-atom cell. The different IT site occupancies correspond to a decrease in the IT–IT distance from 2·62 Å for our IT occupancy of 4Fe+4Zn to 2·47 Å with Johanssen's (1968) IT occupancy of 8 Fe (accepted metallic diameter for Fe $\simeq$ 2·52 Å and for Zn $\simeq$ 2·76 Å). These interatomic distance values confirm the occupancies found in the refinements in each case and support the conclusion that the crystal structures are significantly different although both occur within the established γ Fe–Zn phase boundaries.

During structural studies of these γ phases, it was noted that their atomic packing might be regarded as an approximation to the theoretically unobtainable packing of perfect tetrahedra. A quantitative assessment of this point of view will be presented separately, but it is useful to note here that the γ brass structure does exhibit one feature which is common in other structures that have been interpreted as approximations to tetrahedral packing. One such group of 'tetrahedrally close-packed structures' made up of interpenetrating CN 12 (coordination number = 12), CN 14, CN 15 and/or CN 16 polyhedra can be regarded as having structures generated by the alternate stacking of *main* layer-nets of atoms made up of triangles, pentagons and/or hexagons, and *secondary* layer-nets of atoms made up of triangles and/or squares, with the atoms of the secondary nets lying over the centres of the pentagons or hexagons of the primary nets. The hexagons of one main layer are overlaid antisymmetrically by pentagons or hexagons respectively of the main layers above and below (Frank & Kasper, 1959; Shoemaker & Shoemaker, 1967; Pearson & Shoemaker, 1969). Somewhat similar characteristics also appear for γ brass, when layers parallel to $(0\bar{1}1)$ planes are considered (Fig. 2). A transformation of the γ brass cell $(\mathbf{a},\mathbf{b},\mathbf{c})$ to a new cell $(\mathbf{a}',\mathbf{b}',\mathbf{c}')$, matrix $(100/01\bar{1}/011)$, places these layers on (001) planes of the new cell perpendicular to $[0\bar{1}1]$ of the γ brass cell. A planar pentagon–triangle net (main layer) is found on the mirror plane at $z'=0$ (z' refers to the new cell), and similar rumpled nets occur at $z'\simeq\pm0{\cdot}18$ such that the pentagons of these cover the ones at $z'=0$ antisymmetrically. Between these three layers there are distorted triangular secondary nets of atoms at $z'\simeq\pm0{\cdot}12$ which lie over the centres of the pentagons of the main nets. This sequence of layers is limited to five, since the next triangular layers beyond $z'\simeq0{\cdot}18$ are omitted. The structure continues along [001] of the new cell with another five-layer sequence bounded by layers at $z'\simeq$ 0·32 and 0·68 with a mirror plane at $z'=0{\cdot}5$. This second five-layer sequence is displaced from the position of the first by either $\mathbf{a}'/2$ or $\mathbf{b}'/2$ in the new cell. Hence, Fig. 2 shows that γ brass exhibits certain features characteristic of other structures which have previously been interpreted as examples of distorted tetrahedral packing.

During construction of models of γ brass clusters using spheres of various sizes, it was noted that the OH and CO spheres can lie at positions of metastable equilibrium with regard to their contacts with neighbours in the same cluster. Using equal-sized spheres for example, each OH sphere touches two IT spheres, but it rests mid-way between two OT spheres and does not touch them (see Fig. 3). If the OH sphere were displaced toward either of the OT spheres, it could then touch three spheres in the cluster but this change would destroy the $I\bar{4}3m$ space group symmetry. A variety of other possibilities can arise when IT, OT and OH spheres of different radii are considered. Our data on

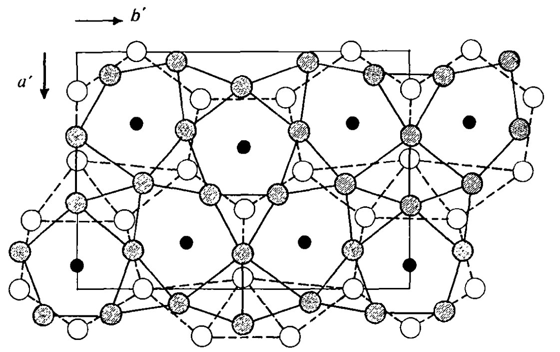

Fig. 2. Layers of atoms on (0$\bar{1}$1) planes of the Fe_3Zn_{10} structure. The layer in full outline is on the mirror plane ($z'=0$ of transposed cell; see text). Layers in broken outline are at $z' \simeq \pm 0{\cdot}18$. Atoms shown near centres of pentagons are at $z' \simeq \pm 0{\cdot}12$.

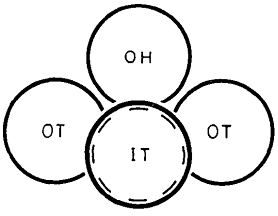

Fig. 3. Illustration of the metastable equilibrium position for an OH site with spheres of equal size. The OH sphere touches two IT spheres above and below the plane of the drawing. The OH sphere could be displaced toward either OT sphere to make an additional contact. CO sites occupy similar metastable positions.

the γ brass structures are not sufficiently accurate to determine whether atoms in the OH positions could be in one such limiting contact position preferentially, in both limiting contact positions equally, or in the central positions entirely. Such features, if present randomly throughout a crystal, may be the origin of relatively high final R values beyond which structure refinement of γ phases appears impossible at present.

In summary, our work confirms to higher accuracy and for a more extensive set of observed data the previously reported crystal structures of Cu_5Zn_8 and Cu_5Cd_8. In the case of Fe_3Zn_{10} a new ordering has been found within the γ phase region and a superstructure was also observed.

We are grateful to Mr V. Fronz for determining the lattice parameters of γ Cu–Cd alloys. The work was made possible through support provided by the National Research Council of Canada.

References

Bradley, A. J. & Gregory, C. H. (1931). *Phil. Mag.* **12**, 143–162.

Bradley, A. J. & Jones, P. (1933). *J. Inst. Met.* **51**, 131–162.

Bradley, A. J. & Thewlis, J. (1926). *Proc. Roy. Soc.* A**112**, 678–692.

Brandon, J. K., Chieh, P. C., Pearson, W. B. & Riley, P. W. (1974). Submitted to *Acta Cryst.*

Frank, F. C. & Kasper, J. S. (1959). *Acta Cryst.* **12**, 483–499.

Hansen, M. (1958). *Constitution of Binary Alloys*, 2nd ed., pp. 415–417. New York: McGraw-Hill.

Heidenstam, O. von, Johansson, A. & Westman, S. (1968). *Acta Chem. Scand.* **22**, 653–661.

International Tables for X-ray Crystallography (1968). Vol. III, 2nd ed., pp. 201–216. Birmingham: Kynoch Press.

Johansson, A., Ljung, H. & Westman, H. (1968). *Acta Chem. Scand.* **22**, 2743–2753.

Johansson, A. & Westgren, A. (1933). *Metallwirtschaft*, **12**, 385–387.

Owen, E. A. & Pickup, L. (1933). *Proc. Roy. Soc.* A**140**, 179–191.

Pearson, W. B. & Shoemaker, C. B. (1969). *Acta Cryst.* B**25**, 1178–1183.

Schramm, J. (1938). *Z. Metallk.* **30**, 122–130.

Shoemaker, C. B. & Shoemaker, D. P. (1967). *Acta Cryst.* **23**, 231–238.

Westgren, A. & Phragmén, G. (1925). *Phil. Mag.* **50**, 311–341.

Westman, S. (1965). *Acta Chem. Scand.* **19**, 1411–1419.